








Article

Physicochemical Properties of a Bioactive Polysaccharide Film from *Cassia grandis* with Immobilized Collagenase from *Streptomyces parvulus* (DPUA/1573)

Kétura Ferreira ¹, Kethylen Cardoso ¹, Romero Brandão-Costa ², Joana T. Martins ³, Cláudia Botelho ³, Anna Neves ⁴, Thiago Nascimento ⁵, Juanize Batista ⁴, Éverton Ferreira ⁶, Fernando Damasceno ⁶, Amanda Sales-Conniff ⁷, Wendell Albuquerque ^{8,*}, Ana Porto ⁴ and José Teixeira ³

- ¹ Postgraduate Program in Biological Applied to Health, Department of Biosciences, Federal University of Pernambuco, Recife 50670-901, Brazil; ketura.cavalcante@ufpe.br (K.F.); kethylen.barbara@ufpe.br (K.C.)
 - ² Institute of Biological Sciences, University of Pernambuco, Recife 50100-130, Brazil; romero.brandao@upe.br
 - ³ CEB—Centre of Biological Engineering (LABBELS—Associate Laboratory), University of Minho, 4710-057 Braga, Portugal; joanamartins@ceb.uminho.pt (J.T.M.); claudiabotelho@deb.uminho.pt (C.B.); jateixeira@deb.uminho.pt (J.T.)
 - ⁴ Department of Animal Morphology and Physiology, Federal Rural of University of Pernambuco, Recife 52171-900, Brazil; anna.dneves@ufrpe.br (A.N.); ana.porto@ufrpe.br (A.P.)
 - ⁵ Campus Professor Cinobelina Elvas, Federal University of Piauí, Bom Jesus 64049-550, Brazil; thiagopajeu@ufpi.edu.br
 - ⁶ Campus Serra da Capivara, Federal University of São Francisco Valley-Univasf, Sao Raimundo Nonato 64770-000, Brazil; everton.franca@univasf.edu.br (É.F.); fernando.damasceno@univasf.edu.br (F.D.)
 - ⁷ USF Health Heart Institute, University of South Florida, 560, Channelside Drive, Tampa, FL 33602, USA; amandasales@usf.edu
 - ⁸ Institute of Food Chemistry and Food Biotechnology, Justus Liebig University Giessen, Heinrich-Buff-Ring 17, 35392 Giessen, Germany
- * Correspondence: wendell.albuquerque@lcb.chemie.uni-giessen.de



Citation: Ferreira, K.; Cardoso, K.; Brandão-Costa, R.; Martins, J.T.; Botelho, C.; Neves, A.; Nascimento, T.; Batista, J.; Ferreira, É.; Damasceno, F.; et al. Physicochemical Properties of a Bioactive Polysaccharide Film from *Cassia grandis* with Immobilized Collagenase from *Streptomyces parvulus* (DPUA/1573). *Cosmetics* **2024**, *11*, 86. <https://doi.org/10.3390/cosmetics11030086>

Academic Editor: Vasil Georgiev

Received: 19 April 2024

Revised: 15 May 2024

Accepted: 20 May 2024

Published: 29 May 2024



Copyright: © 2024 by the authors. Licensee MDPI, Basel, Switzerland. This article is an open access article distributed under the terms and conditions of the Creative Commons Attribution (CC BY) license (<https://creativecommons.org/licenses/by/4.0/>).

Abstract: (1) Background: Polysaccharide films are promising vehicles for the delivery of bioactive agents such as collagenases, as they provide controlled release at the wound site, facilitating tissue regeneration. This study aimed to investigate the physicochemical properties of *Cassia grandis* polysaccharide films with immobilized collagenase from *Streptomyces parvulus* (DPUA/1573). (2) Methods: Galactomannan was extracted from *Cassia grandis* seeds for film production with 0.8% (*w/v*) galactomannan and 0.2% (*v/v*) glycerol with or without collagenases. The films underwent physical-chemical analyses: Fourier-transform infrared spectroscopy (FTIR), scanning electron microscopy (SEM), thermogravimetric analysis (TGA), color and opacity (luminosity-*L*^{*}, green to red-*a*^{*}, yellow to blue-*b*^{*}, opacity-*Y*%), moisture content, water vapor permeability (WVP), thickness, contact angle, and mechanical properties. (3) Results: The results showed similar FTIR spectra to the literature, indicating carbonyl functional groups. Immobilizing bioactive compounds increased surface roughness observed in SEM. TGA indicated a better viability for films with immobilized *S. parvulus* enzymes. Both collagenase-containing and control films exhibited a bright-yellowish color with slight opacity (*Y*%). Mechanical tests revealed decreased rigidity in PCF (−25%) and SCF (−41%) and increased deformability in films with the immobilized bioactive compounds, PCF (234%) and SCF (295%). (4) Conclusions: Polysaccharide-based films are promising biomaterials for controlled composition, biocompatibility, biodegradability, and wound healing, with a potential in pharmacological applications.

Keywords: polysaccharide film; collagenase; *Streptomyces parvulus*; skin healing

1. Introduction

Recent years have witnessed a change in cosmetic research, focusing on improving aesthetics and health benefits such as wound healing [1]. This change has sparked greater interest in investigating natural ingredients with therapeutic properties for skincare, as well as combining various compounds to promote tissue regeneration [2]. The healing process involves dynamic tissue formation to repair damage, with phases determining scar type. The inflammatory phase aims to remove devitalized tissues, the proliferative phase focuses on tissue formation through fibroblast proliferation and collagen production, and the maturation phase involves collagen type replacement, lasting from 6 months to 2 years. Complications can affect scar characteristics [3–7]. Recognizing the vital importance of biodiversity, the international community has established the Sustainable Development Goals (SDGs), including SDG 15, which aims to protect, restore, and promote the sustainable use of terrestrial ecosystems [8,9]. There is a growing demand for sustainable alternatives across various sectors, including the materials industry. Among these alternatives is the use of natural bioactive principles, involving the extraction and utilization of compounds from natural sources such as plants and microorganisms to develop products with diverse applications [10].

Over time, various dressings made from natural polymers have been employed to mitigate the environmental impact of waste and minimize toxicity to patients. These dressings demonstrate adequate permeability, offer antimicrobial protection, and promote accelerated healing without causing cytotoxic effects [8,9]. Additionally, certain polymers play a crucial role in tissue remodeling and re-epithelialization processes during the healing process [8]. In this context, polysaccharides from natural sources have garnered attention for their biocompatibility, biodegradability, and bioactive attributes. *Cassia grandis*, a tropical leguminous plant species, is recognized for harboring polysaccharides that exhibit medicinal promise [10,11]. Referred to as pink cassia, this plant is extensively utilized in traditional medicine and pharmaceutical pursuits [12]. The seeds of *Cassia grandis* contain a gummy endosperm rich in galactomannan, an ecologically sustainable, low-cost, and non-toxic material known for its safety. Galactomannan can be used in solution or gel forms, making it versatile for various applications and facilitating large-scale use. These seeds have the capability to form polysaccharide films, which can encapsulate and release bioactive compounds. Polymeric matrices are valued for their biocompatibility, structural support, and wound-healing properties [13,14].

Polysaccharide films are promising vehicles in delivering bioactive agents such as collagenases, enzymes capable of degrading collagen, which plays a crucial role in tissue remodeling and skin regeneration [15–18]. By incorporating collagenase into the polysaccharide film, it can be released in a controlled manner at the wound site, leading to the degradation of excess collagen and facilitating tissue regeneration, thus minimizing the risk of hypertrophic or keloid scars [19,20]. Therefore, there is an effort to create products and techniques that thoroughly cater to the requirements of wound care while ensuring patient comfort and possessing antimicrobial properties. By combining the benefits of polysaccharide films with the therapeutic properties of collagenases, it is possible to advance towards more effective and personalized therapies for wound treatment, thereby improving the quality of life of patients and promoting safe and efficient healing.

Therefore, this study aimed to incorporate collagenases into polysaccharide films derived from *Cassia grandis* seeds, evaluating their physicochemical and mechanical properties, like thickness, morphology, FTIR, TGA, color, and mechanical properties, and to submit the results through analysis.

2. Materials and Methods

2.1. Materials

Cassia grandis seeds were collected in Recife (PE, Brazil, 8°02'50.0" S 34°57'00.1" W) in April 2022. Ethanol (99.8%), acetone P.A. and sodium chloride were obtained from Vetec Fine Chemicals (Rio de Janeiro, RJ, Brazil), while commercial collagenase (Collagenase

type I) was purchased from Pan Biotech (Worthington, OH, USA), and azocoll from Sigma-Aldrich (St. Louis, MO, USA). All other chemicals were of analytical grade.

2.2. Obtaining Galactomannan

Galactomannan was obtained from *Cassia grandis* seeds, according to Albuquerque et al. [21]. The purification process involved experimenting with *Cassia grandis* pods in distilled water at 25 °C for 18 h. Subsequently, the pods were separated in half, exposing the seeds, which were then removed and dried until they reached a constant weight. The dried seeds were boiled in distilled water in a ratio of 1:5 (*w/v*) at 100 °C for 1 h for enzyme inactivation, and then kept in water for 18 h at 25 °C to facilitate the removal of the shell. Then, the peel was removed and the waste was ground in a blender with 5% (*w/v*) 0.1 M NaCl at 25 °C. The material was then filtered through a tissue and later through a screen printing cloth and precipitated with 46% ethanol in a ratio of 1:3 (*v/v*) for 18 h. The resulting white precipitate was washed with 100% ethanol in a ratio of 1:3 (*w/v*) for 30 min and then twice with acetone in a ratio of 1:3 (*w/v*) for 30 min each and filtered. There was on-screen printing between each wash. The precipitate was then dried until it reached a constant weight, ground and called galactomannan.

2.3. Film Preparation

The film solutions were prepared in distilled water with 0.8% (*w/v*) galactomannan and 0.2% (*v/v*) glycerol, and kept under magnetic stirring (500 rpm) for 18 h at room temperature (20 ± 2 °C). A total of 15 mL of film-forming solutions were deposited in polystyrene Petri dishes with a diameter of 90 mm. The films were then dried in an oven at 33 °C for 9 h and subsequently stored at 20 °C and 54% relative humidity (RH) until further characterization [14].

2.4. Collagenase Produced by *Streptomyces parvulus*

Collagenase was obtained from *Streptomyces parvulus*, isolated from lichens from the Amazon region and belonging to the DPUA 1573 culture collection (Department of Parasitology at the Federal University of Amazonas). The isolated microorganism was maintained in ISP-2 medium [22] with 10% glycerol at −20 °C.

For the production of collagenolytic protease, MS-2 medium [23], pH 7, was autoclaved at 121 °C/1 atm for 20 min. Erlenmeyer flasks (250 mL) containing 100 mL of culture medium were used, with the inoculum corresponding to 10⁸ CFU/mL.

Collagenase activity was performed using the method described by Chavira [24]. The reaction mixture consisted of 50 µL of sample and 950 µL of buffer with 5 mg (mg/L) of Azocoll solution in a 1.0 mL reaction tube and incubated at 37 °C in a water bath for 60 min.

The absorbance of the supernatant was measured at λ550 nm using a UV-VIS spectrophotometer (UV-1900i Shimadzu, Barueri, Brazil). One unit of enzymatic activity (U) was defined as the amount of enzyme per ml of sample that when taken after 60 min of incubation led to an increase in absorbance of 0.001 at λ550 nm, due to the formation of soluble peptides linked by azo dye. Specific activity was calculated as the ratio between the enzymatic activity and the total protein content of the sample and expressed in U/mg.

2.5. Determination of Proteins

The protein content of the samples was determined using the methods of Smith [25], using BCA Kit (Thermo Scientific, Waltham, MA, USA) with bovine serum albumin as a standard. A spectroscopic analysis was conducted using a microplate reader at a wavelength of 562 nm.

2.6. Collagenase Purification

The purification of the protease with collagenolytic activity was based on a two-step procedure. The crude extract was initially precipitated with a 70% concentration of acetone. A precipitated fraction was collected using centrifugation at 10,000 rpm, 4 °C for

20 min. The supernatant was discarded and the pellet was collected and resuspended in the minimum volume of 0.1 M Tris-HCl buffer pH 7.5.

To obtain the protease with collagenolytic activity, anion chromatography was used on QAE-sephadex G-50 resin to separate the protein fractions eluted using Tris-HCl buffer pH 7.5 added with 0.15 M NaCl in a 1.0 × 12 cm. The separation protein profile was evaluated at 215 nm and 280 nm.

2.7. Immobilization of Collagenase in Polysaccharide Film

Commercial collagenase (Collagenase type I—PAN Biotech®) and collagenase obtained from *Streptomyces parvulus* were added to the film-forming solutions (*w/v*) and left under magnetic stirring (500 rpm) for 5 h, at room temperature (20 ± 2 °C). A constant amount (15 mL) of each of the film-forming solutions obtained was molded into a 90 mm diameter polystyrene Petri dish. The films were conditioned in an oven at 33 °C for 9 h and maintained at 20 °C and 54% relative humidity (RH) until further characterization [17].

2.8. Characterization of the Polysaccharide Film and the Film Incorporated with Collagenases

The galactomannan film without the addition of collagenase was called polysaccharide film (PF) and was used as a reference in all analyses. Films with incorporated collagenase were named the following: polysaccharide film with commercial collagenase enzyme (PCF) and polysaccharide film with collagenase obtained from *Streptomyces parvulus* (SCF).

2.8.1. Film Thickness

The film thickness was determined using a digital micrometer (Mitutoyo, Kanagawa, Japan). Five different points were selected at random in each film and the measurement was carried out. The average values obtained from the measurements were used in calculations related to water vapor permeability (WVP) and mechanical properties.

2.8.2. Scanning Electron Microscopy (SEM)

The examination of film surfaces was conducted via scanning electron microscopy (SEM) utilizing a transmission electron microscope (TEM, Hitachi, HT7700, Tokyo, Japan). Each film was affixed to a coverslip with a thin layer of chromium and carbon to prevent the buildup of static charge during electron exposure, thus ensuring accurate scanning without distortions or artifacts. For enhanced visualization, samples underwent sputtering with colloidal gold particles and subsequent drying prior to scanning.

2.8.3. Fourier-Transform Infrared Spectroscopy (FTIR)

Film characterization employed Fourier-transform infrared spectroscopy (FTIR) using a Bruker FT-IR VERTEX 80/80 v spectrometer (Boston, MA, USA) in Attenuated Total Reflectance (ATR) mode, employing a platinum crystal accessory. Analyses covered the frequency range of 400 to 4000 cm⁻¹, with 16 scans and a resolution of 4 cm⁻¹. Before measurement, a background spectrum was obtained from a clean surface. The PF served as the reference, with spectra obtained from films containing incorporated bioactive compounds (PCF and SCF) being subtracted from the PF spectrum. Additionally, a 30 min ultraviolet radiation exposure test was conducted to assess structural changes post-sterilization.

2.8.4. Thermogravimetric Analysis (TGA)

Thermogravimetric analysis (TGA) was performed using a Mettler Toledo TGA/DSC 1, model Star System. Samples underwent heating from 20 °C to 450 °C at a rate of 10 °C min⁻¹ under a nitrogen atmosphere.

2.8.5. Color and Opacity

Color and opacity were evaluated utilizing a digital colorimeter (Konica Minolta, model Chroma Meter CR-400, Osaka, Japan) calibrated at illuminant C with a white standard. Parameters measured included L* (L* = 0 [black] and L* = 100 [white]), a*

($-a^*$ = greenness and $+a^*$ = redness), and b^* ($-b^*$ = blueness and $+b^*$ = yellowness), as recommended by the International Commission on Illumination. Opacity was determined as the ratio of sample opacity on the black standard (Y_b) to its opacity on the white standard (Y_w). Five random measurements each of Y_b and Y_w were averaged for calculation. The experiment was conducted in triplicate, and results were expressed as a percentage: $Y (\%) = (Y_b/Y_w) \times 100$.

2.8.6. Moisture Content

Moisture content (MC) represented the percentage of water removed from the initial sample mass. MC was determined gravimetrically through drying films at 105 °C in an oven with forced air circulation for 24 h. Experiments were performed in triplicate.

2.8.7. Water Vapor Permeability (WVP)

The assessment of water vapor permeability (WVP) was determined gravimetrically based on the ASTM E96-92 method [26,27]. For analysis, it was necessary to seal the film in the upper part of a permeation cell containing distilled water (100% RH; 2337 Pa vapor pressure 20 °C), which was then placed in a desiccator at 20 °C and 0% RH (0 Pa pressure water vapor) containing silica. The cells were weighed at intervals of 2 h for 10 h. Steady-state and uniform water pressure conditions were assumed through maintaining the air circulation constant outside the test cell by using a miniature fan inside the desiccator [28]. The slope of weight loss versus time was obtained using linear regression. Three replicates were obtained for each sample.

2.8.8. Contact Angle

The contact angle was measured on a facial contact angle meter (OCA 20, Data-physics, Filderstadt, Germany). Film samples were taken using a 500 µL syringe (Hamilton, Bonaduz, Switzerland) with a 0.75 mm diameter needle. Pure water was used to measure the layer between the surface and the liquid. The contact angle on the film surfaces was measured using the sessile drop method [29]. Measurements were taken for 15 s.

2.8.9. Mechanical Properties

The mechanical properties were verified using a TA-HD plus texture analyzer (Serial RS232, Stable Micro Systems, Surrey, UK) according to ASTM D 882-02 (2010) guidelines. According to the ASTM standard, film strips with a length of 100 mm and a width of 20 mm were used and the average film thickness was measured beforehand. The initial gripper separation was set at 100 mm and the crosshead speed was set at 5 mm min⁻¹.

2.8.10. Statistical Analysis

Statistical analyses were performed using standard deviation of triplicate assays. Data were analyzed using one-way analysis of variants (ANOVA or Kruskal–Wallis test) using the free software RStudio (version 2023.12.1+402). Significant differences were verified using Tukey's test or Dunn's test based on post hoc multiple comparisons, with a significance level defined at a p value < 0.05.

3. Results

3.1. Scanning Electron Microscopy (SEM)

Figure 1 compares the surface morphology of the galactomannan-based film without the incorporation of the bioactive compound (a1–a3), with the galactomannan-based film with commercial collagenase enzyme at 0.1% incorporated (b1–b3) and the galactomannan-based film with collagenolytic enzyme for *Streptomyces parvulus* (c1–c3). The images obtained were magnified at 100×, 250× and 1000×.

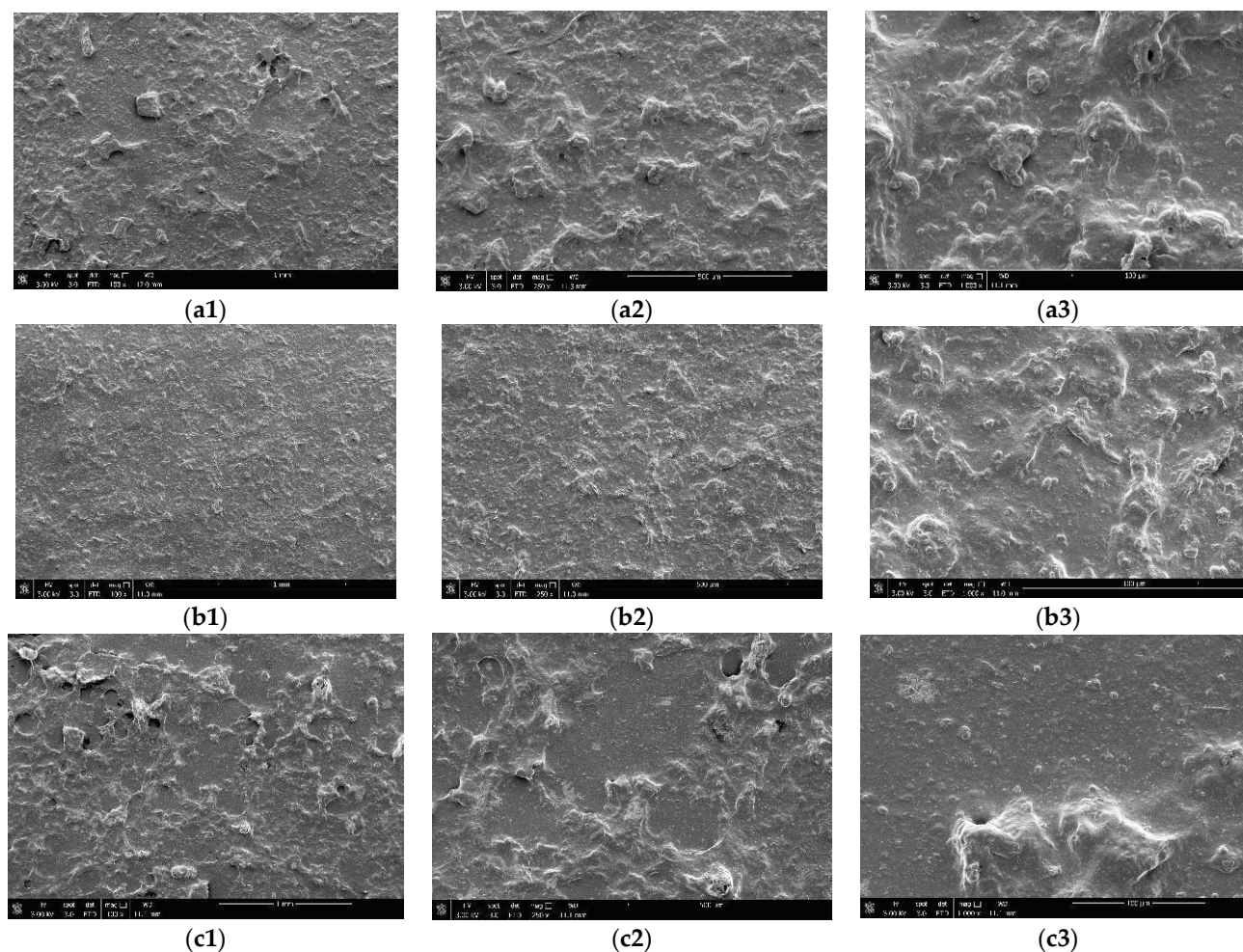


Figure 1. SEM images showing the surface structure of galactomannan film with and without bioactive compound incorporations. (a1–a3) 100× magnitude; (b1–b3) 250× magnitude; (c1–c3) 1000× magnitude.

3.2. Thickness and Moisture Content

The film thickness was not affected by the incorporation of enzymes, as shown in Table 1. Regarding MC, the samples were similar. There was no significant difference (p value = 0.0729) between the moisture content of the galactomannan-based film with 0.1% commercial collagenase enzyme incorporated and the galactomannan-based film with collagenolytic enzyme for *Streptomyces parvulus*. But both films with collagenase had a higher moisture content than the polymer film without the incorporation of bioactive compounds.

Table 1. Thickness and moisture content for the polysaccharide films before and after immobilization (values expressed as average \pm standard deviation).

Films	Thickness (nm)	Moisture Content (%)
PF	0.0718 ± 0.0325^a	$54 \pm 5 \times 10^{-5}^a$
PCF	0.0528 ± 0.0104^a	$23.56 \pm 0.0009^{b,c}$
SCF	0.0698 ± 0.0123^a	13.15 ± 0.0009^c

^{a–c} Mean values in the same column indicated with different letters are significantly different (p value < 0.05). Those that have the same letter in the same column are not significantly different (p value > 0.05).

3.3. Water Vapor Permeability (WVP)

The analysis of water vapor permeability in polysaccharide films involves studying the interaction of water vapor with these films to understand their properties. In Figure 2, the water vapor permeability in PF, PCF, and SCF is observed.

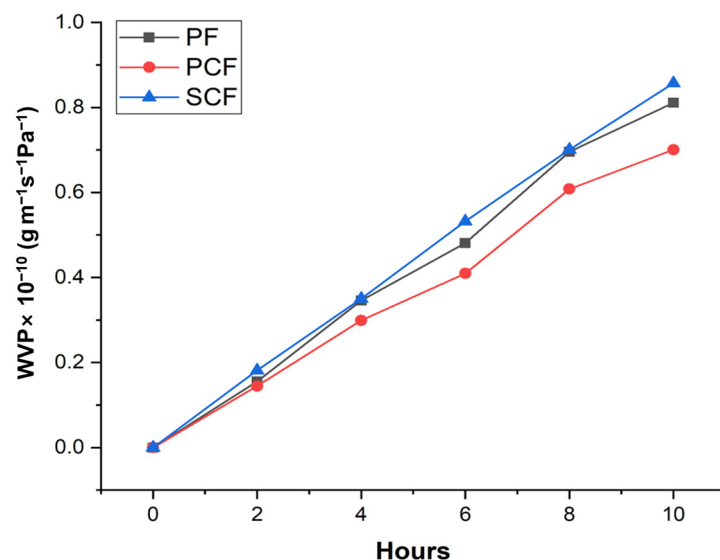


Figure 2. Variation in effective coefficients for WVP in polysaccharide films related to relative humidity at 20 °C.

3.4. Contact Angle before and after Ultraviolet Radiation

The contact angle pre- and post-ultraviolet irradiation can be observed in Table 2. It is derived from the film's surface and serves as a straightforward and efficient method for assessing the films' hydrophobicity level.

Table 2. Contact angle for the polysaccharide films before and after immobilization with enzymes (values expressed as average \pm standard deviation).

Films	Water Contact Angle (°)	
	Without Exposure to UV	After Exposure to UV
PF	77.9 \pm 1.56 ^a	91.1 \pm 1.25 ^a
PCF	58.0 \pm 2.55 ^b	64.8 \pm 2.49 ^b
SCF	92.77 \pm 1.83 ^c	136.1 \pm 2.43 ^c

^{a-c} Mean values in the same column indicated with different letters are significantly different (p value < 0.05). Those that have the same letter in the same column are not significantly different (p value > 0.05).

3.5. Fourier-Transform Infrared Spectroscopy (FTIR)

Fourier-transform infrared spectroscopy (FTIR) is a technique used to obtain information about chemical composition and molecular structure, based on the interaction between molecules with infrared radiation. FTIR was used to investigate possible chemical interactions between the galactomannan-based film and collagenases, in both the commercial (PCF) and the collagenase produced using *Streptomyces parvulus* (SCF).

Figure 3 shows the spectra of the polysaccharide films after the incorporation of commercial collagenase and collagenase produced using *Streptomyces parvulus*. A wide range of band stretching was observed in the FTIR spectra of the galactomannan film, ranging from 3324 cm⁻¹ to 687 cm⁻¹. Stretching in the region of 3030–3600 cm⁻¹ is attributed to OH⁻¹ groups, indicating the presence of carbohydrates and a small amount of moisture. Furthermore, bands at 2904 cm⁻¹ and 1024 cm⁻¹ suggest C-H stretching and a C-O bond from the alcohol group, respectively. The stretching observed at 2904 cm⁻¹ and in the range of 1000–1200 cm⁻¹ suggests characteristic features of carbohydrate polymers. Additionally,

the presence of amides at 1634 cm^{-1} confirms the existence of proteins in the galactomannan sample. In the IR spectra of galactomannan, bands were observed at 808 cm^{-1} and 874 cm^{-1} , which are associated with the occurrence of anomeric configurations (CH oscillations of α and β conformers) and glycosidic linkages. These bands are attributed to α -D-galactopyranose units and β -D-mannopyranose units, respectively.

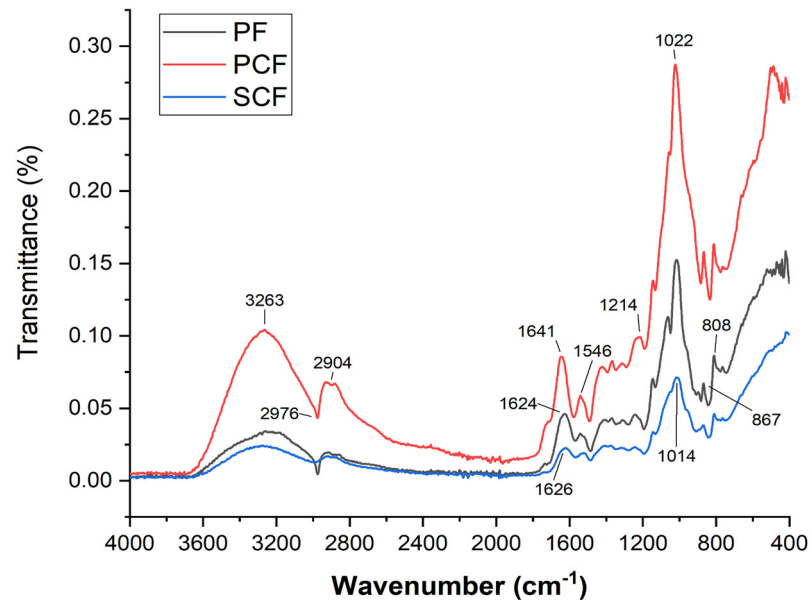
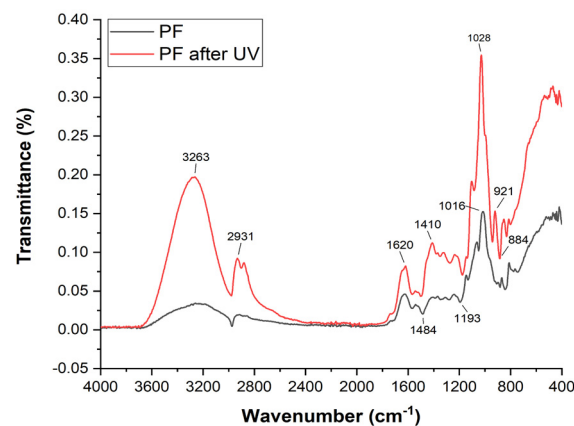


Figure 3. FTIR Spectra of the polysaccharide films after the incorporation of commercial collagenase enzymes and collagenase produced using *Streptomyces parvulus*.

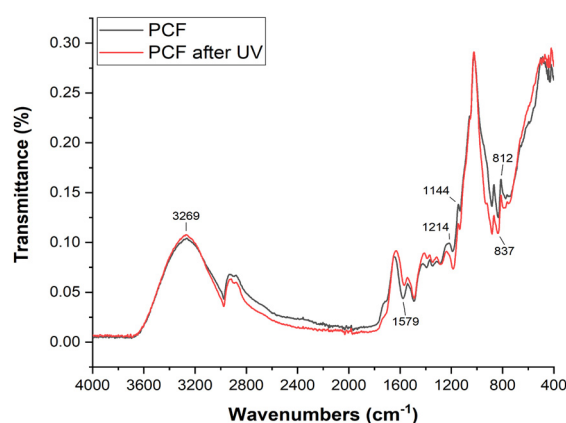
The absence of the band above 3000 cm^{-1} suggests an interaction of the OH groups with the glycine of collagen. Other signals indicative of the incorporation of collagenase into the polysaccharide film are observed. Notably, bands at 1626 cm^{-1} , characteristic of C=O stretching typical of amide I, and at 1546 cm^{-1} and 1294 cm^{-1} , typical of N-H bending and C-N stretching of amide II, respectively, are identified. Additionally, signals at 1459 cm^{-1} , characteristic of pyrrolidine rings, amide III, which were not present in the galactomannan film previously, are observed.

Figure 4 shows the spectra of the polysaccharide films after exposure to ultraviolet radiation, so that it would be possible to observe whether there are differences in the composition and structure of the film if subjected to radiation.

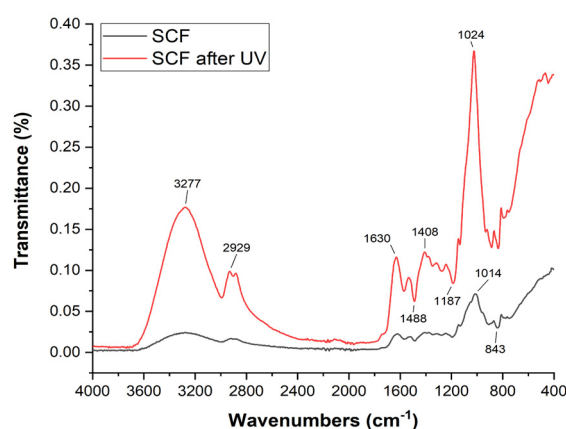


(a)

Figure 4. Cont.



(b)



(c)

Figure 4. FTIR Spectra (before and after UV exposure) of the polysaccharide films (a) polysaccharide film with commercial collagenase enzyme (b) and polysaccharide film with collagenase produced using *Streptomyces parvulus* (c).

3.6. Thermogravimetric Analysis (TGA)

Thermogravimetric analysis (TGA) is a technique used to measure weight changes in a sample material due to time or temperature. TGA can be used to analyze the thermal stability of films and determine the presence of moisture and composition-related details. The thermal degradation results for the films are shown in Figure 5.

In the PF (Figure 5a), this event corresponds to a mass loss of 13%. A second event is observed with the onset around 188 °C (band at 292 °C), with a mass loss of about 60%. This event is related to the film's decomposition process. The width of the peak in the TGA curve suggests that the decomposition process is complex. The glycerol used in the film should initiate its decomposition before the polysaccharide chain (shoulders at a temperature close to 240 °C), while the peak at 292 °C is related to the polysaccharide decomposition. In the film incorporated with commercial enzymes (PCF, Figure 5b), this initial event corresponds to a mass loss of 8%. A second event is observed starting at 185 °C (peak at 294 °C) and is related to the decomposition process of the polysaccharide chain of the film. Once again, the width of the peak suggests the occurrence of simultaneous events, with the decomposition of glycerol occurring at a lower temperature than the polysaccharide chain. The mass loss throughout the entire event is 58.5%.

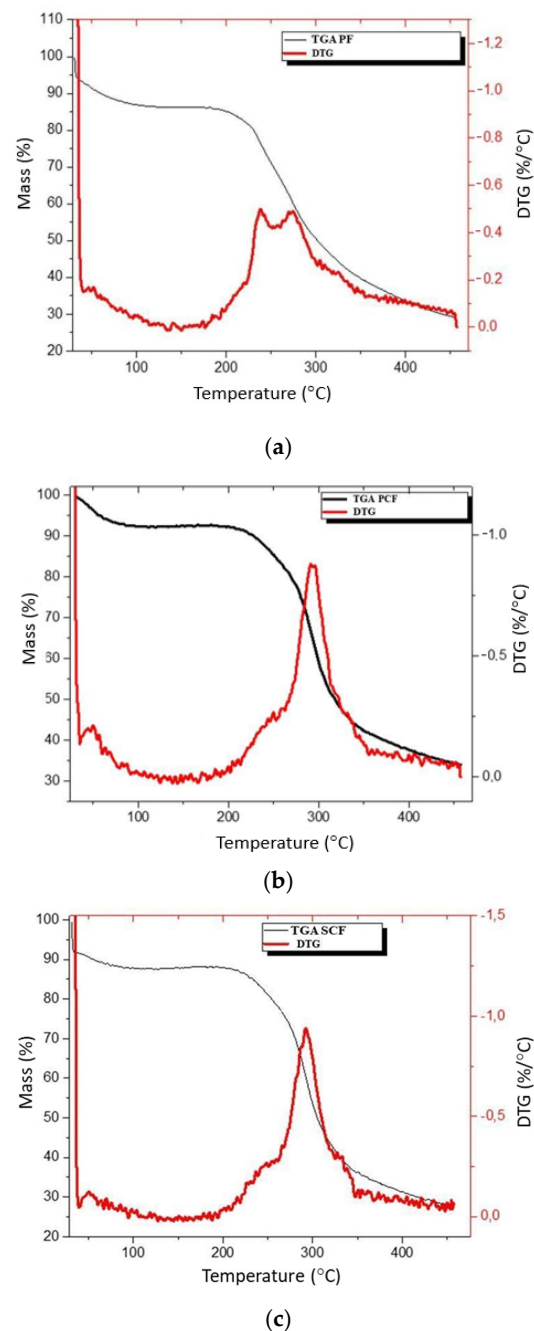


Figure 5. Thermogravimetric analysis of the polycarbohydrate films (a), polycarbohydrate film with commercial collagenase enzyme (b) and polycarbohydrate film with collagenase produced using *Streptomyces parvulus* (c).

As for the film with enzymes obtained from *Streptomyces parvulus* (SCF, Figure 5c), the mass loss corresponding to the first event is about 14%, a value consistent with the previous samples. The second event, starting at 173 °C, is related to the onset of the thermal decomposition process of the film. The total mass loss throughout the second event is 55.8%. The TGA curve shows two distinct peaks, the first with a maximum of 237 °C and the second with a maximum of 273 °C. The first peak should be related to the decomposition process of glycerol, while the second peak is related to the decomposition process of the polycarbohydrate chain of the film.

3.7. Color and Opacity

In pharmaceutical products, color and transparency play pivotal roles in consumer acceptance. Table 3 illustrates the color characteristics and transparency of the films. Notably, all examined films displayed distinct luminosity, primarily reflected in their L* coordinate values, alongside a discernible hint of yellowness denoted by the b* coordinate. Furthermore, all films exhibited slight opacity with no significant discrepancies observed among them (Figure 6).

Table 3. Color parameters L* (luminosity), a* (−a* = greenness and +a* = redness), b* (−b* = blueness and +b* = yellowness) and Y (opacity) for the polysaccharide films before and after immobilization (values expressed as average ± standard deviation).

Films	L*	a*	b*	Y (%)
PF	96.20 ± 0.1426 ^a	0.68 ± 0.0262 ^a	6.63 ± 0.2412 ^a	13.41 ± 0.1988 ^a
PCF	94.11 ± 0.2217 ^{a,b}	0.85 ± 0.0355 ^b	9.94 ± 0.2687 ^a	13.53 ± 0.2992 ^a
SCF	93.71 ± 0.2490 ^b	1.08 ± 0.0852 ^c	6.54 ± 0.2638 ^a	13.63 ± 0.2343 ^a

^{a–c} Mean values in the same column indicated with different letters are significantly different (*p* value < 0.05). Those that have the same letter in the same column are not significantly different (*p* value > 0.05).

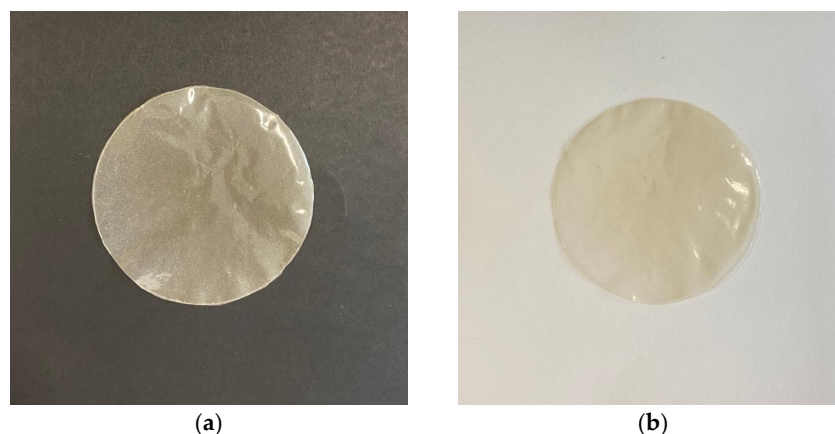


Figure 6. Representative image of the galactomannan film with immobilized collagenase obtained *Streptomyces parvulus* on black (a) and white (b) background.

3.8. Mechanical Properties

Table 4 shows the mechanical properties (Young's modulus—YM, tensile strength—TS and elongation at break—EB) of the galactomannan films without and with immobilized bioactive compounds (Table 4).

Table 4. Effect of concentration on Young's modulus (YM), tensile strength (TS) and elongation at break (EB) of the films (*w/v*) films before and after immobilization of collagenases in the film-forming mixture.

Films	YM (Mpa)	TS (Mpa)	EB (%)
PF	3.76 ± 0.145 ^a	2.29 ± 0.505 ^a	0.855 ± 0.095 ^a
PCF	4.7 ± 0.12 ^{b,c}	7.65 ± 0.450 ^{b,c}	1.015 ± 0.195 ^a
SCF	5.335 ± 0.145 ^c	9.05 ± 0.850 ^c	1.010 ± 0.200 ^a

^{a–c} Mean values in the same column indicated with different letters are significantly different (*p* value < 0.05). Those that have the same letter in the same column are not significantly different (*p* value > 0.05).

4. Discussion

4.1. Scanning Electron Microscopy (SEM)

The scanning electron microscopy (SEM) results provide valuable insights into the surface morphology of galactomannan-based films under different conditions. It is possible

to observe in the images generated using SEM some residual granules from the extraction of galactomannan. According to Arruda et al. [30] NaCl is used to enhance the solubility of free proteins and ethanol and acetone are used to wash out contaminants and proteins. Despite these steps in the present study, the film still had visible deformities. Deformities in polymeric films after the incorporation of biomolecules can vary based on the specific techniques and materials used. Research has shown that polymer films can exhibit significant changes in physical and mechanical properties when doped with biological molecules [31]. For example, the adsorption of proteins such as fibronectin can be influenced by the type of dopant used, affecting the binding to proteins on the film surface [32]. Furthermore, studies have demonstrated that polymer films can be deformed through the adsorption/desorption of molecules, leading to rapid and substantial changes in elasticity [33].

It is noted that the film containing commercial collagenase presented a smaller number of granules when compared to the film containing collagenase produced using *Streptomyces parvulus*. Enzymes designed for commercial use are often optimized for specific applications and may exhibit a high degree of substrate specificity. This could influence the enzymatic activity on the galactomannan matrix, affecting the formation and distribution of granules [34]; in parallel, the collagenases from *Streptomyces parvulus* interact with a wider range of components in the galactomannan matrix, leading to a more diverse and perhaps uneven distribution of granules [8].

As stated by Cerqueira et al. [35], when carrying out a study with and without the incorporation of extracts into galactomannan films, it was evident in the films with extract incorporation that there are some granular, spherical vesicles apparently free of visible fissures and pores. It is possible to observe in the results that the films with the incorporation of the enzymes present an inhomogeneous distribution in the film matrix. In the study by Albuquerque et al. [17], the presence of granules was observed depending on the type of biomolecule that was incorporated. Therefore, the distribution and characteristics of granules in films appear to be influenced by the nature of the incorporated enzymes and biomolecules.

4.2. Thickness and Moisture Content

The thickness of polysaccharide films with incorporated compounds can be influenced by several factors. Beloglazova et al. [36] observed that the concentration of polysaccharides influenced the appearance and thickness of the films. Cado et al. [37] reported that the simultaneous spraying of chitosan, hyaluronic acid and alginate resulted in a linear increase in thickness with spraying time.

Ramudu et al. [38] states in their study that the grain size increases the film thickness, which differs from the present study. The thickness of galactomannan films with enzymes varies depending on the specific enzyme and the conditions of the immobilization process; however, there was no significant difference between the incorporated and free films.

The moisture content in a film can affect the physical and chemical properties, being a key parameter when choosing a film for specific applications [39,40]. Enzymes can interact with the chemical structure of the film once incorporated, which can lead to changes in its hydrophilic/hydrophobic balance [41]. In the present study, a decrease in MC values was observed in the films with collagenolytic enzymes, especially those obtained from *Streptomyces parvulus*. Antoniou et al. [42] claimed that films with compounds such as enzymes have a more compact structure, which allows them to occupy more volume in the polymer matrix, reducing MC values. Slade et al. [43] highlights that the incorporation of enzymes into films can lead to a decrease in moisture content. It has also been observed that the enzymatic degradation of cellulose films results in a thinner and more diluted interfacial film, leading to a decrease in interfacial mass over time [44]. Ahmadi et al. [45], Cerqueira et al. [46], Ghasemlou et al. [47], and Albuquerque et al. [17] report that the distribution and proportion of galactose units along the mannan chain may play a fundamental role in the water content of galactomannans.

4.3. Water Vapor Permeability (WVP)

The water vapor permeability of polysaccharide films can be influenced by the irregular surface of the film, as visualized in the SEM (Figure 1), which could act as a site for water binding during moisture absorption, thus allowing water vapor to pass through the film [48,49]. Salgado et al. [50], in their study, observed that the addition of micro/nano clays or Cloisite 30B to polysaccharide-based films can affect their mechanical and barrier properties, influencing both WVP and tensile strength. Cerqueira et al. [51] reported that the hydrophobicity induced through incorporating corn oil into films can alter the film matrix's affinity with water, subsequently affecting WVP and mechanical properties.

These findings collectively suggest that the surface characteristics of polysaccharide films play a crucial role in determining their WVP and overall barrier performance, highlighting the importance of surface modifications to control moisture absorption and vapor transmission through the film. Regarding the differences between PF and PCF films, it was observed that there were few, suggesting that the permeability of the film is not significantly affected by commercial collagenase. It is believed that the SCF film presents a greater difference due to its purification condition; as can be seen in Figure 1, there is still the presence of several granules indicating that the PCF presents greater purity.

The values reported in our study demonstrated that the SCF, in addition to interacting with the galactomannan film, affected the WVP. Water vapor permeability in a film containing *Cassia grandis* polysaccharide with immobilized enzymes can be influenced by various factors. Polysaccharide films from the *Cassia fistula* seed present that increasing glycerol concentration in the film increased water vapor permeability [43]. Moreover, enzymes are immobilized in carriers with water-soluble polymeric substances, forming thin films on the carrier's surface, which involves removing water from the polymer during immobilization. [51]. In addition, porous polysaccharide-based biopolymers can be designed to have high porosity, allowing water vapor to pass through their pores or matrix and increasing the bioavailability of the bioactive compound [52]; the incorporation of biomolecules into these films can further increase their porosity and consequently their WVP. These findings suggest that the water vapor permeability of a film with *Cassia grandis* polysaccharide and immobilized enzyme are modulated via the film's composition and structure, impacting its suitability for different applications.

4.4. Contact Angle before and after Ultraviolet Radiation

As the angular values increase, they indicate the presence of a higher hydrophobic surface [48,49]. Surfaces with contact angles below 90° are considered hydrophilic. From the static sessile drop method with ultrapure water, the observed contact angles appear to be more hydrophilic in PF and PCF, while SCF is more hydrophobic than the others ($p > 0.05$) with a contact angle $> 90^\circ$. *Streptomyces parvulus* collagenase may have higher hydrophobicity than commercial collagenases due to differences in composition and purification. Despite these variations, it still shows sufficient activity and does not affect the usability of the polysaccharide film. Hence, it is a reliable option for making films with healing properties, providing a promising alternative in producing biodegradable and bioactive materials for different uses.

The contact angle of polysaccharide films containing enzymes can be significantly influenced by various factors, such as ultraviolet (UV) radiation. UV irradiation can alter the contact angle and surface properties of biopolymeric films, leading to changes in surface roughness and polarity [53]. Furthermore, Zimoch-Korzycka et al. [54] reported that the presence of enzymes such as cellulase in polysaccharide films can impact their physicochemical stability over time, affecting parameters such as water vapor permeability and tensile strength. Xu et al. [53] found that UV irradiation exposure decreases water contact angles in certain polymer films, attributed to the formation and release of surfactants from irradiated surfaces.

The polarity characteristics of the polymeric surface can modulate the interaction with proteins and the cell surface at the time of its application [55]. Therefore, the contact angle

of polysaccharide films with enzymes can vary before and after UV radiation, influenced by the specific enzymes present and the effects of UV radiation on the film surfaces [56].

4.5. Fourier-Transform Infrared Spectroscopy (FTIR)

The free galactomannan film presented a similar spectrum as obtained by Albuquerque et al. [21], corroborating that the film originates from polysaccharide from *Cassia grandis* seeds.

Exposure to UV rays leads to various effects like breaking bonds [57], oxidizing groups, and altering polysaccharide and enzyme structures [58]. Research has shown that the exposure to UV radiation has the potential to induce alterations in the FTIR of collagen-derived films through a decrease in the concentration of amino acids within the collagen structure, thereby influencing the overall composition of the film [59]. Despite showing differences in intensity, Figure 4 shows few differences perceived in the bands presented, indicating a reasonable resistance of the film to degradation caused by UV radiation.

4.6. Thermogravimetric Analysis (TGA)

All films demonstrated mass loss due to thermal degradation. Mass loss occurs due to the loss of moisture, the evaporation of water and glycerol, and finally, the decomposition of the polysaccharide, similar to the results obtained by Albuquerque et al. [17]. The experiments carried out in this study are in accordance with those reported in the literature [30,45], indicating specific interactions between film components and enzymes [60], especially between the enzyme obtained from *Streptomyces parvulus* (SCF) which demonstrated slightly better performance compared to the commercial enzyme (PCF) and pure polysaccharide film (PF) in terms of thermal behavior. Panda, Park and Seo [61] highlight the ability to incorporate materials of organic origin to provide greater thermal stability, which corroborates the current study.

4.7. Color and Opacity

The color and opacity of polysaccharide films can be crucial for various applications, especially when incorporating enzymes. Cerclier et al. [62] introduced a method using cellulose nanocrystals and xyloglucan to detect enzymatic activity through color changes in thin films. Kim et al. [63] focused on increasing the opacity of laccase-based time-temperature integrators by incorporating TiO₂ and xanthan gum, while maintaining the color change kinetics.

By strategically combining different components, polysaccharide films can achieve improvements in opacity and color stability for various applications. According to Diaz-Montes [64], the utilization of natural polysaccharides, plasticizers, metallic ions and bioactive compounds may result in enhanced mechanical, barrier, and optical characteristics. Moreover, concerning Figure 6, it is emphasized that at a macroscopic level, the SPC film exhibits robust structural integrity, thus indicating its suitability for industrial utilization and commercial viability.

4.8. Mechanical Properties

YM is a measure of sample stiffness and a decrease in this value indicates a reduction in film rigidity, leading to increased film deformability [65]. PF was significantly different from PCF ($p = 0.034$) and SCF ($p = 0.008$), but there was no significant difference between PCF and SCF; in other words, the immobilization of bioactive compounds improves the film's resistance. TS refers to the maximum tensile stress that the film can withstand. This parameter is closely linked to the chemical structure of the film and is strongly influenced by its composition, including water, plasticizers, surfactants, and bioactive compounds immobilized in the film matrix [66]. PF was significantly different from PCF ($p = 0.018$) and SCF ($p = 0.009$), but there was no significant difference between PCF and SCF regarding TS. EB, which refers to the film's flexibility, did not show any significant difference between any of the films ($p > 0.05$).

The mechanical properties of polysaccharide films can be significantly influenced by various factors, such as manufacturing techniques, composition, and additives [67]. Zhang et al. [68] observed that the incorporation of phenolic acids into soluble soy polysaccharide films increased antioxidant and antibacterial properties while also affecting mechanical strength and water vapor barrier properties. Fu et al. [69], in their study with films made from corn starch and *Tremella fuciformis* polysaccharide, demonstrated varied mechanical properties based on the proportion of components. Lazo et al. [70] observed that polysaccharide films derived from chañar fruit polysaccharides showed good mechanical properties, thermal stability, and biodegradability, making them suitable for various applications.

5. Conclusions

The outcomes elucidated in this investigation support the conclusion that the use of polysaccharide films derived from the *Cassia grandis* plant, whether in their pure form or combined with bioactive enzymes, represents a promising approach for application in wound management and tissue rejuvenation, with potential implications reaching into the realms of healthcare and the cosmetic industry. The analysis using scanning electron microscopy unveiled variations in the surface morphology of the films, thus verifying the presence of specific interactions between polysaccharides and enzymes, potentially impacting the distribution and development of granules. Furthermore, the films exhibited uniform thickness and moisture content attributes, with the permeability to water vapor being dependent on both the film composition and the characteristics of the enzymes incorporated within. Films containing enzymes derived from *Streptomyces parvulus* (SCF) and films with commercial enzymes showed no significant difference, but it is highlighted that the collagenase obtained from SP is easier to obtain using fermentation methods, underscoring the significance of the enzyme origin in the formulation of these films. The findings also revealed variations in contact angles, indicating differing hydrophobicity levels among the films with potential implications for surface properties and interactions. Moreover, the Fourier-transform infrared spectroscopy (FTIR) analysis provided insights into chemical interactions between the films and enzymes, with UV radiation demonstrating minimal effects on the film composition. Additionally, thermogravimetric analysis (TGA) highlighted differences in thermal behavior, suggesting variations in the degradation process influenced by enzyme incorporation. The authors highlight the significance of this research as a crucial milestone in the analysis of the film, with promising implications for future experiments in different scenarios.

Author Contributions: K.F.—Conceptualization, methodology, investigation, data curation, writing—original draft preparation, writing, review and editing; K.C.—conceptualization, data curation, writing, review and editing; R.B.-C.—writing, review and editing, supervision, project administration and funding acquisition; J.T.M.—methodology, investigation and supervision; C.B.—methodology, investigation and supervision; A.N.—writing, review, validation and formal analysis; T.N.—writing, review and editing; J.B.—writing, review and editing; É.F.—formal analysis, writing and editing; F.D.—formal analysis, writing and editing; A.S.-C.—review and editing; W.A.—formal analysis, Review and editing; A.P.—supervision, project administration and funding acquisition; J.T.—supervision, project administration and funding acquisition. All authors have read and agreed to the published version of the manuscript.

Funding: This work was supported by Foundation for Science and Technology Development of the State of Pernambuco (FACEPE) (IBPG-1491-2.08/19), by National Council for Scientific and Technological Development (CNPq) (200501/2022-4), by Portuguese Foundation for Science and Technology (FCT) under the scope of the strategic funding of UIDB/04469/2020 unit, by LABBELS—Associate Laboratory in Biotechnology, Bioengineering and Microelectromechanical Systems (LA/P/0029/2020), by program Marie Skłodowska-Curie grant (MSCA-RISE; FODIAC; 778388), and by the European Regional Development Fund (ERDF) through the Competitiveness factors Operational program—Norte 2020, COMPETE.

Institutional Review Board Statement: Not applicable.

Informed Consent Statement: Not applicable.

Data Availability Statement: The original contributions presented in the study are included in the article, further inquiries can be directed to the corresponding author.

Conflicts of Interest: The authors declare no conflicts of interest.

References

1. Fadilah, N.I.M.; Phang, S.J.; Kamaruzaman, N.; Salleh, A.; Zawani, M.; Sanyal, A.; Maarof, M.; Fauzi, M.B. Antioxidant biomaterials in cutaneous wound healing and tissue regeneration: A critical review. *Antioxidants* **2023**, *12*, 787. [[CrossRef](#)]
2. Xiao, H.; Chen, X.; Liu, X.; Wen, G.; Yu, Y. Recent advances in decellularized biomaterials for wound healing. *Mater. Today Bio* **2023**, *19*, 100589. [[CrossRef](#)] [[PubMed](#)]
3. Prabhu, S.R. Healing: Tissue Regeneration and Repair. In *Textbook of General Pathology for Dental Students*; Springer Nature: Cham, Switzerland, 2023; pp. 49–56. [[CrossRef](#)]
4. Gomes, B.S.; Do Bomfim, F.R.C.; de Jesus Lopes Filho, G. Photobiomodulation in the skin healing process-literature review Photobiomodulation in wound healing process-literature review. *Braz. J. Dev.* **2020**, *6*, 66814–66826. [[CrossRef](#)]
5. Balbino, C.A.; Pereira, L.M.; Curi, R. Mechanisms involved in wound healing: A revision. *Rev. Bras. Ciências Farm.* **2005**, *41*, 27–51. [[CrossRef](#)]
6. Ferreira, C.M.; D'Assumpção, E.A. Cicatrizes hipertróficas e queloides. *Rev. Soc. Bras. Cir. Plást* **2006**, *21*, 40–48.
7. Potter, D.A.; Veitch, D.; Johnston, G.A. Scarring and wound healing. *Br. J. Hosp. Med.* **2019**, *80*, C166–C171. [[CrossRef](#)] [[PubMed](#)]
8. Arora, P. Life below land: The need for a new sustainable development goal. *Front. Environ. Sci.* **2023**, *11*, 1215282. [[CrossRef](#)]
9. Valladares, F. More biodiversity to improve our health: The benefits to human well-being of favouring functional and diverse ecosystems. *Metode Sci. Stud. J.* **2023**, *13*, 111–117. [[CrossRef](#)]
10. Ponphaiboon, J.; Krongrawa, W.; Aung, W.W.; Chinatangkul, N.; Limmatvapirat, S.; Limmatvapirat, C. Advances in natural product extraction techniques, electrospun fiber fabrication, and the integration of experimental design: A comprehensive review. *Molecules* **2023**, *28*, 5163. [[CrossRef](#)]
11. Costa, E.P.; Brandão-Costa, R.M.P.; Albuquerque, W.W.C.; Nascimento, T.P.; Sales Conniff, A.E.; Cardoso, K.B.B.; Neves, A.G.D.; Batista, J.M.S.; Porto, A.L.F. Extracellular collagenase isolated from *Streptomyces antibioticus* UFPEDA 3421: Purification and biochemical characterization. *Prep. Biochem. Biotechnol.* **2024**, *54*, 260–271. [[CrossRef](#)]
12. Sheokand, B.; Vats, M.; Kumar, A.; Srivastava, C.M.; Bahadur, I.; Pathak, S.R. Natural polymers used in the dressing materials for wound healing: Past, present and future. *J. Polym. Sci.* **2023**, *61*, 1389–1414. [[CrossRef](#)]
13. Koshy, J.T.; Vasudevan, D.; Sangeetha, D.; Prabu, A.A. Biopolymer Based Multifunctional Films Loaded with Anthocyanin Rich Floral Extract and ZnO Nano Particles for Smart Packaging and Wound Healing Applications. *Polymers* **2023**, *15*, 2372. [[CrossRef](#)]
14. Fuentes, J.A.M.; Fernández, I.M.; Fernández, H.Z.; Sánchez, J.L.; Alemán, R.S.; Navarro-Alarcon, M.; Borrás-Linares, I.; Maldonado, S.A.S. Quantification of bioactive molecules, minerals and bromatological analysis in ficarao (*Cassia grandis*). *J. Agric. Sci.* **2020**, *12*, 88. [[CrossRef](#)]
15. Raikwar, S.; Bidla, P.D.; Jain, A.; Jain, S.K. Plant polysaccharides-based nanoparticles for drug delivery. In *Plant Polysaccharides as Pharmaceutical Excipients*; Elsevier: Amsterdam, The Netherlands, 2022. [[CrossRef](#)]
16. Alhawarri, M.B.; Dianita, R.; Rawa, M.S.A.; Nogawa, T.; Wahab, H.A. Potential Anti-Cholinesterase Activity of Bioactive Compounds Extracted from *Cassia grandis* Lf and *Cassia timoriensis* DC. *Plants* **2023**, *12*, 344. [[CrossRef](#)] [[PubMed](#)]
17. Albuquerque, P.B.S.D. Avaliação Reológica da Galactomanana Extraída das Sementes de *Cassia grandis*. Master's Thesis, Universidade Federal de Pernambuco, Recife, Brazil, 2013.
18. Albuquerque, P.B.S.; Soares, P.A.G.; Aragão-Neto, A.C.; Albuquerque, G.S.; Silva, L.C.N.; Lima-Ribeiro, M.H.M.; Silva Neto, J.C.; Coelho, L.C.B.B.; Correia, M.T.S.; Teixeira, J.A.C.; et al. Healing activity evaluation of the galactomannan film obtained from *Cassia grandis* seeds with immobilized *Cratylia mollis* seed lectin. *Int. J. Biol. Macromol.* **2017**, *102*, 749–757. [[CrossRef](#)]
19. Oliveira, V.M.; Cunha, M.N.C.; Assis, C.R.D.; Nascimento, T.P.; Herculano, P.N.; Holanda, M.T.; Porto, A.L.F. Colagenases do pescado e suas aplicações industriais. *Pubvet* **2017**, *11*, 243–255. [[CrossRef](#)]
20. Ferreira, I.A.A.; de Albuquerque Wanderley, M.C.; Porto, A.L.F. Primeiro relato de produção de collagenase por fungo isolado do solo da Caatinga-Rhizopus microsporus UCP 1296. *Res. Soc. Dev.* **2022**, *11*, e398111234618. [[CrossRef](#)]
21. Albuquerque, P.B.; Barros, W., Jr.; Santos, G.R.; Correia, M.T.; Mourão, P.A.; Teixeira, J.A.; Carneiro-da-Cunha, M.G. Characterization and rheological study of the galactomannan extracted from seeds of *Cassia grandis*. *Carbohydr. Polym.* **2014**, *104*, 127–134. [[CrossRef](#)]
22. Pridham, T.G.; Aderson, P.; Foley, C. Selection of media for maintenance and taxonomic study of *Streptomyces*. *Antibiot. Ann.* **1957**, 947–953. [[PubMed](#)]
23. Porto, A.L.F.; Campos-Takaki, G.M.; Lima Filho, J.L. Effects of culture conditions on protease production by *Streptomyces clavuligerus* growing on the soy bean flour medium. *Appl. Biochem. Biotechnol.* **1996**, *60*, 115–122. [[CrossRef](#)]
24. Chavira, R., Jr.; Burnett, T.J.; Hageman, J.H. Assaying proteinases with azocoll. *Anal. Biochem.* **1984**, *136*, 446–450. [[CrossRef](#)] [[PubMed](#)]
25. Smith, P.E.; Krohn, R.I.; Hermanson, G.T.; Mallia, A.K.; Gartner, F.H.; Provenzano, M.; Fujimoto, E.K.; Goeke, N.M.; Olson, B.J.; Klenk, D.C. Measurement of protein using bicinchoninic acid. *Anal. Biochem.* **1985**, *150*, 76–85. [[CrossRef](#)] [[PubMed](#)]

26. Gontard, N.; Duchez, C.; Cuq, B.; Guilbert, S. Edible composite films of wheat gluten and lipids: Water vapour permeability and other physical properties. *Int. J. Food Sci. Technol.* **1994**, *29*, 39–50. [[CrossRef](#)]
27. McHugh, T.H.; Avena-Bustillos, R.; Krochta, J.M. Hydrophilic edible films: Modified procedure for water vapor permeability and explanation of thickness effects. *J. Food Sci.* **1993**, *58*, 899–903. [[CrossRef](#)]
28. Guillard, V.; Broyart, B.; Bonazzi, C.; Guilbert, S.; Gontard, N. Preventing moisture transfer in a composite food using edible films: Experimental and mathematical study. *J. Food Sci.* **2003**, *68*, 2267–2277. [[CrossRef](#)]
29. Kwok, D.Y.; Neumann, A.W. Contact angle measurement and contact angle interpretation. *Adv. Colloid Interface Sci.* **1999**, *81*, 167–249. [[CrossRef](#)]
30. Arruda, I.R.; Albuquerque, P.B.; Santos, G.R.; Silva, A.G.; Mourão, P.A.; Correia, M.T.; Vicente, A.A.; Carneiro-da-Cunha, M.G. Structure and rheological properties of a xyloglucan extracted from *Hymenaea courbaril* var. *courbaril* seeds. *Int. J. Biol. Macromol.* **2015**, *73*, 31–38. [[CrossRef](#)]
31. Zhao, Y.; Ganapathysubramanian, B.; Shrotriya, P. Cantilever deflection associated with hybridization of monomolecular DNA film. *J. Appl. Phys.* **2012**, *111*, 074310. [[CrossRef](#)]
32. Ikawa, T.; Hoshino, F.; Matsuyama, T.; Takahashi, H.; Watanabe, O. Molecular-shape imprinting and immobilization of biomolecules on a polymer containing azo dye. *Langmuir* **2006**, *22*, 2747–2753. [[CrossRef](#)]
33. Okuzaki, H. A biomorphic origami actuator fabricated by folding a conducting paper. *J. Phys.* **2008**, *127*, 012001. [[CrossRef](#)]
34. Kunzendorf, A.; Bornscheuer, U.T. Optimierte Designer-Enzyme für die pharmazeutische Industrie. *BIOspektrum* **2022**, *28*, 760–762. [[CrossRef](#)]
35. Cerqueira, M.A.; Souza, B.W.; Martins, J.T.; Teixeira, J.A.; Vicente, A.A. Seed extracts of *Gleditsia triacanthos*: Functional properties evaluation and incorporation into galactomannan films. *Food Res. Int.* **2010**, *43*, 2031–2038. [[CrossRef](#)]
36. Beloglazova, C.E.; Rysmukhambetova, G.E.; Karpunina, L.V.; Zabelina, M.V. Development of a technology for polysaccharide-based film coating. *IOP Conf. Ser. Earth Environ. Sci.* **2021**, *640*, 052022. [[CrossRef](#)]
37. Cado, G.; Kerdjoudj, H.; Chassepot, A.; Lefort, M.; Benmlih, K.; Hemmerle, J.; Voegel, J.-C.; Jierry, L.; Schaaf, P.; Frère, Y.; et al. Polysaccharide films built by simultaneous or alternate spray: A rapid way to engineer biomaterial surfaces. *Langmuir* **2012**, *28*, 8470–8478. [[CrossRef](#)] [[PubMed](#)]
38. Ramudu, M.; Raja, M.M.; Basumatary, H.; Kamat, S.V. Role of film thickness on magnetic properties of sputter deposited Co₂FeGa alloy thin films. *Mater. Res. Express* **2019**, *6*, 086404. [[CrossRef](#)]
39. Lad, S.; Narkhede, S.; Luhar, S.; Prajapati, A. Review on Moisture Content: A stability problem in pharmaceuticals. *EPRA Int. J. Res. Dev. (IJRD)* **2022**, *7*, 27–33. [[CrossRef](#)]
40. Vishnevskiy, A.S.; Seregin, D.S.; Vorotilov, K.A.; Sigov, A.S.; Mogilnikov, K.P.; Baklanov, M.R. Effect of water content on the structural properties of porous methyl-modified silicate films. *J. Sol-Gel Sci. Technol.* **2019**, *92*, 273–281. [[CrossRef](#)]
41. Ohayon, D.; Renn, D.; Wustoni, S.; Guo, K.; Druet, V.; Hama, A.; Chen, X.; Maria, I.P.; Singh, S.; Griggs, S.; et al. Interactions of catalytic enzymes with n-type polymers for high-performance metabolite sensors. *ACS Appl. Mater. Interfaces* **2023**, *15*, 9726–9739. [[CrossRef](#)]
42. Antoniou, J.; Liu, F.; Majeed, H.; Zhong, F. Characterization of tara gum edible films incorporated with bulk chitosan and chitosan nanoparticles: A comparative study. *Food Hydrocoll.* **2015**, *44*, 309–319. [[CrossRef](#)]
43. Slade, L.; Levine, H.; Wang, M.; Ievolella, J. DSC Analysis of Starch Thermal Properties Related to Functionality in Low-Moisture Baked Goods. In *New Techniques in the Analysis of Foods*; Tunick, M.H., Palumbo, S.A., Fratamico, P.M., Eds.; Springer: Boston, MA, USA, 1998. [[CrossRef](#)]
44. Lee, D.M.; Sims, J.L. Water Soluble Compositions Incorporating Enzymes, and Method of Making Same. U.S. Patent US20130244920A1, 19 September 2013.
45. Ahmadi, R.; Kalbasi-Ashtari, A.; Oromiehie, A.; Yarmand, M.S.; Jahandideh, F. Development and characterization of a novel biodegradable edible film obtained from psyllium seed (*Plantago ovata* Forsk.). *J. Food Eng.* **2012**, *109*, 745–751. [[CrossRef](#)]
46. Cerqueira, M.A.; Souza, B.W.; Teixeira, J.A.; Vicente, A.A. Effect of glycerol and corn oil on physicochemical properties of polysaccharide films—A comparative study. *Food Hydrocoll.* **2012**, *27*, 175–184. [[CrossRef](#)]
47. Ghasemlou, M.; Khodaiyan, F.; Oromiehie, A. Physical, mechanical, barrier, and thermal properties of polyol-plasticized biodegradable edible film made from kefir. *Carbohydr. Polym.* **2011**, *84*, 477–483. [[CrossRef](#)]
48. Ubeyitogullari, A.; Ahmadzadeh, S.; Kandhola, G.; Kim, J. Polysaccharide-based porous biopolymers for enhanced bioaccessibility and bioavailability of bioactive food compounds: Challenges, advances, and opportunities. *Compr. Rev. Food Sci. Food Saf.* **2022**, *21*, 4610–4639. [[CrossRef](#)] [[PubMed](#)]
49. Shogren, R. Water vapor permeability of biodegradable polymers. *J. Environ. Polym. Degr.* **1997**, *5*, 91–95. [[CrossRef](#)]
50. Salgado, D.; Serment-Moreno, V.; Ulloa, P.A.; Velazquez, G.; Antonio Torres, J.; Welti-Chanes, J. Steady and unsteady-state determination of the water vapor permeance (wvp) of polyethylene film to estimate the moisture gain of packed dry mango. *Food Bioprocess Technol.* **2017**, *10*, 1792–1797. [[CrossRef](#)]
51. Cerqueira, M.A.; Vicente, A.A. Reinforcement of Polysaccharide-based films: Evaluation of Physic-chemical Properties. In Proceedings of the International Conference Eco-Sustainable Food Packaging Based on Polymer Nanomaterials (Book of Abstracts), Rome, Italy, 26–28 February 2014; ISBN 978-889-808-545-3. Available online: <https://hdl.handle.net/1822/32868> (accessed on 15 March 2024).

52. Sharma, A.; Thatai, K.S.; Kuthiala, T.; Singh, G.; Arya, S.K. Employment of polysaccharides in enzyme immobilization. *React. Funct. Polym.* **2021**, *167*, 105005. [[CrossRef](#)]
53. Xu, Z.; Zhang, Y.; Wang, X.; Li, K.; He, Q. Influence of contact angle on droplet parameters in ellipsoidal wettability model. *Surf. Topogr. Metrol. Prop.* **2023**, *11*, 025022. [[CrossRef](#)]
54. Zimoch-Korzycka, A.; Ambrozik-Haba, J.; Kulig, D.; Jarmoluk, A. Modification effect of cellulase on the physicochemical characteristic of polysaccharides edible films. *Int. J. Polym. Sci.* **2015**, *2015*, 184616. [[CrossRef](#)]
55. Ma, Q.; Hu, D.; Wang, H.; Wang, L. Tara gum edible film incorporated with oleic acid. *Food Hydrocoll.* **2016**, *56*, 127–133. [[CrossRef](#)]
56. Sionkowska, A. UV light as a tool for surface modification of polymeric biomaterials. *Key Eng. Mater.* **2014**, *583*, 80–86. [[CrossRef](#)]
57. Johnson, P.S.; Cook, P.L.; Liu, X.; Yang, W.; Bai, Y.; Abbott, N.L.; Himpel, F.J. Universal mechanism for breaking amide bonds by ionizing radiation. *J. Chem. Phys.* **2011**, *135*, 044702. [[CrossRef](#)]
58. Mieczkowska, A.; Mabilieu, G. Validation of Fourier Transform Infrared Microspectroscopy for the Evaluation of Enzymatic Cross-Linking of Bone Collagen. *Calcif. Tissue Int.* **2023**, *113*, 344–353. [[CrossRef](#)]
59. Moreno, V.; Meroño, C.; Baeza, A.; Usategui, A.; Ortiz-Romero, P.L.; Pablos, J.L.; Vallet-Regí, M. UVA-Degradable Collagenase Nanocapsules as a Potential Treatment for Fibrotic Diseases. *Pharmaceutics* **2021**, *13*, 499. [[CrossRef](#)]
60. Singh, M.K.; Singh, A. Thermogravimetric analyzer. In *Characterization of Polymers and Fibres*; Woodhead Publishing: Cambridge, UK, 2022; pp. 223–240. ISBN 9780128239865. [[CrossRef](#)]
61. Panda, P.K.; Park, K.; Seo, J. Development of poly (vinyl alcohol)/regenerated chitosan blend film with superior barrier, antioxidant, and antibacterial properties. *Prog. Org. Coat.* **2023**, *183*, 107749. [[CrossRef](#)]
62. Cerclier, C.; Guyomard-Lack, A.; Moreau, C.; Cousin, F.; Beury, N.; Bonnin, E.; Jean, B.; Cathala, B. Coloured semi-reflective thin films for biomass-hydrolyzing enzyme detection. *Adv. Mater.* **2011**, *23*, 3791–3795. [[CrossRef](#)]
63. Kim, H.C.; Cha, H.J.; Shin, D.U.; Koo, Y.K.; Cho, H.W.; Lee, S.J. Visibility Enhancement of Laccase-Based Time Temperature Integrator Color by Increasing Opacity. *Korean J. Packag. Sci. Technol.* **2021**, *27*, 101–107. [[CrossRef](#)]
64. Díaz-Montes, E. Polysaccharides: Sources, Characteristics, Properties, and Their Application in Biodegradable Films. *Polysaccharides* **2022**, *3*, 480–501. [[CrossRef](#)]
65. Colombi, P.; Bergese, P.; Bontempi, E.; Borgese, L.; Federici, S.; Keller, S.S.; Boisen, A.; Depero, L.E. Sensitive determination of the Young's modulus of thin films by polymeric microcantilevers. *Meas. Sci. Technol.* **2013**, *24*, 125603. [[CrossRef](#)]
66. Gläßer, T.; Stache, P.; Zschehyge, M. TS-Moulding—Fertigungstechnologie zur großserientauglichen Herstellung endlosfaserverstärkter Thermoplastsandwichstrukturen/TS-Molding—Manufacturing technology for mass production of continuous fiber-reinforced thermoplastic sandwich structures. *Konstruktion* **2021**, *74*, 54–59. [[CrossRef](#)]
67. Sagawa, T.; Nikaido, Y.; Iijima, K.; Sakaguchi, M.; Yataka, Y.; Hashizume, M. Preparation of Mechanically Anisotropic Polysaccharide Composite Films Using Roll-Press Techniques. *ACS Omega* **2023**, *8*, 5607–5616. [[CrossRef](#)]
68. Zhang, M.; Huang, C.; Xie, J.; Shao, Z.; Li, X.; Bian, X.; Xue, B.; Gan, J.; Sun, T. Physical, Mechanical and Biological Properties of Phenolic Acid-Grafted Soluble Soybean Polysaccharide Films. *Foods* **2022**, *11*, 3747. [[CrossRef](#)] [[PubMed](#)]
69. Fu, Z.Q.; Guo, S.X.; Wang, X.Y.; Huang, Z.G.; Bi, C.H.; Li, F.F.; Wu, M. Structural, thermal, mechanical, and physicochemical properties of corn starch and tremella fuciformis polysaccharide based composite films. *Starch-Stärke* **2022**, *74*, 2100255. [[CrossRef](#)]
70. Lazo, L.; Melo, G.M.; Auad, M.L.; Filippa, M.; Masuelli, M.A. Synthesis and Characterization of Chanar Gum Films. *Colloids Interfaces* **2022**, *6*, 10. [[CrossRef](#)]

Disclaimer/Publisher's Note: The statements, opinions and data contained in all publications are solely those of the individual author(s) and contributor(s) and not of MDPI and/or the editor(s). MDPI and/or the editor(s) disclaim responsibility for any injury to people or property resulting from any ideas, methods, instructions or products referred to in the content.